

Cite this: *Chem. Sci.*, 2021, 12, 632

All publication charges for this article have been paid for by the Royal Society of Chemistry

## Cooperative activating effects of metal ion and Brønsted acid on a metal oxo species†

Gui Chen,<sup>a</sup> Li Ma,<sup>b</sup> Po-Kam Lo,<sup>c</sup> Chi-Keung Mak,<sup>\*c</sup> Kai-Chung Lau<sup>id</sup> <sup>\*c</sup> and Tai-Chu Lau<sup>id</sup> <sup>\*c</sup>

Metal oxo (M=O) complexes are common oxidants in chemical and biological systems. The use of Lewis acids to activate metal oxo species has attracted great interest in recent years, especially after the discovery of the CaMn<sub>4</sub>O<sub>5</sub> cluster in the oxygen-evolving centre of photosystem II. Strong Lewis acids such as Sc<sup>3+</sup> and BF<sub>3</sub>, as well as strong Brønsted acids such as H<sub>2</sub>SO<sub>4</sub> and CF<sub>3</sub>SO<sub>3</sub>H, are commonly used to activate metal oxo species. In this work, we demonstrate that relatively weak Lewis acids such as Ca<sup>2+</sup> and other group 2 metal ions, as well as weak Brønsted acids such as CH<sub>3</sub>CO<sub>2</sub>H, can readily activate the stable RuO<sub>4</sub><sup>-</sup> complex towards the oxidation of alkanes. Notably, the use of Ca<sup>2+</sup> and CH<sub>3</sub>CO<sub>2</sub>H together produces a remarkable cooperative effect on RuO<sub>4</sub><sup>-</sup>, resulting in a much more efficient oxidant. DFT calculations show that Ca<sup>2+</sup> and CH<sub>3</sub>CO<sub>2</sub>H can bind to two oxo ligands to form a chelate ring. This results in substantial lowering of the barrier for hydrogen atom abstraction from cyclohexane.

Received 27th July 2020  
Accepted 20th October 2020

DOI: 10.1039/d0sc04069j

rsc.li/chemical-science

### Introduction

High-valent metal oxo (M=O) complexes are common oxidants in the chemical laboratory and in biological systems. Brønsted acids have long been used to increase the oxidizing power of M=O *via* protonation of the oxo ligand (M=O + HX → M–OH<sup>+</sup> + X<sup>-</sup>). However, in recent years, the use of Lewis acids (LA) such as metal ions and boranes to activate M=O has received tremendous attention (M=O + LA → M=O–LA).<sup>1–3</sup> In particular, the interest in understanding the interaction of Lewis acids with metal oxos is stimulated by the discovery that the oxygen-evolving center (OEC) of photosystem II (PSII) is composed of a CaMn<sub>3</sub>O<sub>4</sub> cubane and a dangling Mn linked *via* two μ-oxos.<sup>4–10</sup> A possible role of Ca<sup>2+</sup> is to function as a Lewis acid to modulate the redox reactivity of the manganese oxo complexes.

Strong Lewis acids such as BF<sub>3</sub> and Sc<sup>3+</sup> are usually used to activate metal oxo species. For example, we have reported that the oxidation of alkanes by MnO<sub>4</sub><sup>-</sup> is accelerated by over seven orders of magnitude in the presence of BF<sub>3</sub>.<sup>11</sup> The strong Lewis acid Sc<sup>3+</sup> and the strong Brønsted acid CF<sub>3</sub>SO<sub>3</sub>H have been used

to activate Fe(IV) and Mn(IV) oxo complexes,<sup>12,13</sup> as well as metal superoxo species.<sup>14,15</sup>

There is also much interest in the use of the relatively weak Lewis acid, Ca<sup>2+</sup>, to activate M=O because of its relevance to the CaMn<sub>4</sub>O<sub>5</sub> cluster in Photosystem II; although as expected, its effect is usually much smaller than those of Sc<sup>3+</sup> or BF<sub>3</sub>. For example, Agapie *et al.* reported that Ca<sup>2+</sup> and other metal ions can increase the reduction potentials (*E*<sup>0</sup>) of manganese oxo clusters, and there is a linear correlation between *E*<sup>0</sup> and p*K*<sub>a</sub> of the metal ions.<sup>16,17</sup> Ca<sup>2+</sup> can also enhance the catalytic water oxidation activity of manganese oxides<sup>18,19</sup> and induce the oxidative release of O<sub>2</sub> from a non-heme iron peroxo complex.<sup>20</sup> We have also recently reported that Ca<sup>2+</sup> can increase the rate of oxidation of alcohols by MnO<sub>4</sub><sup>-</sup> (ref. 21) and induce intermolecular O–O coupling of FeO<sub>4</sub><sup>2-</sup> to give O<sub>2</sub>.<sup>22</sup> So far, significant activating effects of Ca<sup>2+</sup> are only reported on metal oxo complexes that are thermodynamically strong oxidants. On the other hand, there has been little or no report on the activation of metal oxo species by weak Brønsted acids such as alkanolic acids.

We have been investigating the effects of Lewis acids on the reactivity of simple metal oxo species bearing two or more oxos without bulky ancillary ligands.<sup>11,21–25</sup> In this type of systems, more than one oxo sites are available for binding to two or more metal ions or Brønsted acids. We report herein the activation of a stable metal oxo complex, RuO<sub>4</sub><sup>-</sup>, by weak Lewis acids such as Ca<sup>2+</sup> and other group II ions, as well as by weak Brønsted acids such as CH<sub>3</sub>CO<sub>2</sub>H. Although iron oxo complexes are common oxidants in chemical and biological systems, they are usually relatively unstable. Hence, we choose to investigate a very stable ruthenium oxo species. Although in a high oxidation state of

<sup>a</sup>Dongguan Cleaner Production Technology Center, School of Environment and Civil Engineering, Dongguan University of Technology, Dongguan, Guangdong 523808, China

<sup>b</sup>Department of Chemistry, Jinan University, Guangzhou, 510632, China

<sup>c</sup>Department of Chemistry, City University of Hong Kong, Tat Chee Avenue, Kowloon Tong, Hong Kong, China. E-mail: bhtclau@cityu.edu.hk; kaichung@cityu.edu.hk; chikmak6@cityu.edu.hk

† Electronic supplementary information (ESI) available. See DOI: 10.1039/d0sc04069j



+VII,  $\text{RuO}_4^-$  is a mild oxidant that readily oxidizes alcohols but is inactive towards alkanes. However, in the presence of a few equiv. of group 2 metal ions or acetic acid, it readily oxidizes cyclohexane at ambient conditions. Notably, the use of  $\text{Ca}^{2+}$  and  $\text{CH}_3\text{CO}_2\text{H}$  together produces a remarkable cooperative effect on  $\text{RuO}_4^-$ , resulting in a much more efficient oxidant than the use of a strong Lewis acid in the presence or absence of a Brønsted acid.

## Results and discussion

### Effects of Lewis acids on oxidation of cyclohexane by $\text{Ru}^{\text{VIII}}\text{O}_4$ and $\text{Ru}^{\text{VII}}\text{O}_4^-$

Tetraoxo complexes of ruthenium in oxidation states +VIII and +VII are known, with  $\text{Ru}^{\text{VIII}}\text{O}_4$  being a much stronger oxidant than  $\text{Ru}^{\text{VII}}\text{O}_4^-$ . As a comparison, we have initially chosen to study the effects of Brønsted and Lewis acids (metal ions and  $\text{BF}_3$ ) on the oxidation of alkanes by  $\text{RuO}_4$ .  $\text{RuO}_4$  is a strong oxidant that is known to oxidize alkanes slowly at room temperature.<sup>26</sup> In our hands, when  $\text{RuO}_4$  (0.01 M) was treated with an excess of cyclohexane (1.0 M) in  $\text{CH}_3\text{CN}$ , 0.2 mol of cyclohexanone/mol of  $\text{RuO}_4$  (20 mol%) was produced after 5 h at 23 °C, as analysed by GC and GC/MS (Fig. 1a and Table S1†). No cyclohexanol could be detected. Since we previously reported that the oxidation of alkanes by  $\text{MnO}_4^-$  is greatly enhanced by just a few equiv. of  $\text{BF}_3$ ,<sup>11</sup> we attempted to do the same with  $\text{RuO}_4$ . However, when  $\text{BF}_3$  was added to  $\text{RuO}_4$ , no enhancement in the rate of cyclohexane oxidation was observed; on the contrary, a lower yield of cyclohexanone (11 mol%) was obtained (Fig. 1a and Table S1†). We then examined if  $\text{Ca}^{2+}$  can activate  $\text{RuO}_4$ , but virtually no effect on cyclohexane oxidation was observed when a few equiv. of  $\text{Ca}(\text{OTf})_2$  ( $\text{OTf}$  is  $\text{CF}_3\text{SO}_3^-$ ) was added. We also tried to activate  $\text{RuO}_4$  with Brønsted acids such as  $\text{CF}_3\text{SO}_3\text{H}$  and  $\text{CH}_3\text{CO}_2\text{H}$  ( $\text{AcOH}$ ), but again there were no effects. These results indicate that the oxo ligands in the highly electrophilic  $\text{RuO}_4$  have little or no affinity for  $\text{CH}_3\text{CO}_2\text{H}$  and various Lewis acids.

On the other hand,  $\text{RuO}_4^-$  is a much weaker oxidant than  $\text{RuO}_4$ ; it is known to oxidize alcohols but not alkanes.<sup>27</sup> When we treated  $[\text{Pr}_4\text{N}][\text{RuO}_4^-]$  with cyclohexane in  $\text{CH}_3\text{CN}$ , no product could be detected after 5 days at 23 °C. Electrospray ionization mass spectrometry (ESI/MS) of the solution after 5 days shows that  $\text{RuO}_4^-$  and  ${}^n\text{Pr}_4\text{N}^+$  are the only species present.



Fig. 1 Time traces for cyclohexane oxidation by (a)  $\text{RuO}_4/\text{Lewis acid}$  and (b)  $\text{RuO}_4^-/\text{Lewis acid}$  in  $\text{CH}_3\text{CN}$ . Conditions:  $\text{RuO}_4$  or  $[\text{Pr}_4\text{N}][\text{RuO}_4^-]$  (0.01 M), Lewis acid (0.04 M), cyclohexane (1.0 M) at 23 °C.

The UV/Vis spectrum of the solution also remained unchanged after 5 days. However, upon adding 4 equiv. of  $\text{BF}_3$  to  $[\text{Pr}_4\text{N}][\text{RuO}_4^-]$  in  $\text{CH}_3\text{CN}$ , 10 mol% of cyclohexanone was produced within 3 h at 23 °C (Fig. 1b and Table S2†). Again, no cyclohexanol product could be detected. More significantly,  $\text{Ca}(\text{OTf})_2$  is also able to activate  $\text{RuO}_4^-$ , and a higher yield of 14 mol% of cyclohexanone was attained (Fig. 1b, S1 and Table S2†). As will be described below, the  $\text{RuO}_4^-/\text{Ca}^{2+}$  system functions as one-electron oxidant, and since the oxidation of cyclohexane to cyclohexanone is a four-electron process, the actual yield is 56%. Other group II metal ions were also found to activate  $\text{RuO}_4^-$ , with cyclohexanone production ranging from 11 to 15 mol% (Fig. 2, Table S2†). The relatively strong Lewis acid  $\text{Sc}(\text{OTf})_3$  was also used and it gave the highest amount of 23 mol% of cyclohexanone. The rate and yield decrease in the order of  $\text{Sc}^{3+}$  ( $\text{p}K_a = 4.3$ ) >  $\text{Mg}^{2+}$  (11.2) >  $\text{Ca}^{2+}$  (12.7) >  $\text{Sr}^{2+}$  (13.2) >>  $\text{Ba}^{2+}$  (13.4); this trend correlates with their  $\text{p}K_a$  values in  $\text{H}_2\text{O}$ , which is a measure of their Lewis acidity.<sup>28</sup> These results indicate that the oxo ligands in  $\text{RuO}_4^-$  are much more basic than those in  $\text{RuO}_4$ , so they readily bind to Lewis acids. Electron-withdrawing by the Lewis acids *via* the oxo ligand enhances the oxidizing power of  $\text{RuO}_4^-$ .

### Kinetics of the oxidation of cyclohexane by $\text{RuO}_4^-/\text{Ca}^{2+}$

The initial rate for cyclohexanone production by  $[\text{Pr}_4\text{N}][\text{RuO}_4^-]$  increases with  $[\text{Ca}^{2+}]$  but eventually levels off at  $[\text{Ca}^{2+}] > 5 \text{ mM}$  (Fig. 3a). A plot of  $1/(\text{initial rate})$  versus  $1/[\text{Ca}(\text{OTf})_2]$  is linear (Fig. 3b). In addition, when the concentration of  $\text{RuO}_4^-$  was doubled, the initial rate was also doubled. Such a kinetic behavior can be represented by eqn (1) and (2). The reacting calcium species is proposed to be  $\text{Ca}(\text{OTf})^+$ , as supported by results of DFT calculations described below. The initial rate of the reaction is shown in eqn (3).



$$\text{Initial rate} = \frac{kK[\text{Ca}(\text{OTf})_2]}{1 + K[\text{Ca}(\text{OTf})_2]} [\text{RuO}_4^-][\text{c} - \text{C}_6\text{H}_{12}] \quad (3)$$



Fig. 2 Effects of various Lewis acids on cyclohexane oxidation by  $\text{RuO}_4^-$  in  $\text{CH}_3\text{CN}$ . Conditions:  $[\text{Pr}_4\text{N}][\text{RuO}_4^-]$  (0.01 M), Lewis acid (0.04 M), cyclohexane (1.0 M) at 23 °C.





Fig. 3 Effects of  $[\text{Ca}(\text{OTf})_2]$  on cyclohexane oxidation by  $\text{RuO}_4^-$  in  $\text{CH}_3\text{CN}$ . Conditions:  $[\text{Pr}_4\text{N}][\text{RuO}_4]$  (0.01 M), cyclohexane (1.0 M) in  $\text{CH}_3\text{CN}$  at 23 °C. (a) Plot of initial rate vs.  $[\text{Ca}(\text{OTf})_2]$ . (b) Plot of  $1/\text{initial rate}$  vs.  $1/[\text{Ca}(\text{OTf})_2]$  (slope =  $(3.16 \pm 0.15) \times 10^3$ , y-intercept =  $(2.16 \pm 0.06) \times 10^6$ ,  $r = 0.988$ ).

From Fig. 3b,  $k = 1/(\text{intercept} [\text{RuO}_4^-]) = (4.63 \pm 0.13) \times 10^{-5} \text{ M}^{-1} \text{ s}^{-1}$  and  $K = \text{intercept/slope} = (6.83 \pm 0.18) \times 10^2 \text{ M}^{-1}$  at 23 °C. The observed equilibrium constant  $K$  indicates relatively strong binding of  $\text{Ca}(\text{OTf})^+$  to  $\text{RuO}_4^-$ , in accordance with the observed rate saturation behaviour.

#### Activation of $\text{RuO}_4^-$ by Brønsted acids

The effects of Brønsted acids on cyclohexane oxidation by  $\text{RuO}_4^-$  were also investigated. Addition of 1 equiv. of the strong acid  $\text{CF}_3\text{SO}_3\text{H}$  ( $\text{p}K_a = 0.23$  in  $\text{H}_2\text{O}$ ) to  $[\text{Pr}_4\text{N}][\text{RuO}_4]$  (0.01 M) in  $\text{CH}_3\text{CN}$  containing excess cyclohexane led to the formation of 15 mol% of cyclohexanone after 3 h at 23 °C. However, addition of  $\geq 4$  equiv. of  $\text{CF}_3\text{SO}_3\text{H}$  to  $[\text{Pr}_4\text{N}][\text{RuO}_4]$  resulted to rapid formation of a black precipitate with only a trace amount of cyclohexanone. Such a phenomenon is due to disproportionation of  $\text{RuO}_4^-$ , as represented by eqn (4).<sup>29</sup>



Interestingly,  $[\text{Pr}_4\text{N}][\text{RuO}_4]$  is also readily activated by the relatively weak acid  $\text{CH}_3\text{CO}_2\text{H}$  ( $\text{p}K_a = 4.76$ ) to oxidize cyclohexane to cyclohexanone, with no evidence of disproportionation even in the presence of high concentrations of  $\text{AcOH}$  ( $>1$  M). Upon addition of 12–48 equiv. of  $\text{AcOH}$  to  $[\text{Pr}_4\text{N}][\text{RuO}_4]$  in  $\text{CH}_3\text{CN}$  containing excess cyclohexane, the brown solution gradually turned green, and 16 mol% of cyclohexanone was produced within 1–2 h at 23 °C. The oxidation state of the ruthenium product was determined to be +6 (see below, Fig. S2†), hence the actual yield is 64%. Although the yield is independent of  $[\text{AcOH}]$ , the rate of oxidation increases with increasing  $[\text{AcOH}]$  (Fig. 4); a plot of the initial rate versus  $[\text{AcOH}]$  gives a straight line. The initial rate is also doubled when  $[\text{RuO}_4^-]$  is doubled. A proposed reaction scheme is shown in eqn (5)–(7). The first step involves protonation of an oxo ligand of  $\text{RuO}_4^-$  by  $\text{AcOH}$ , this step is supported by DFT calculations described below. The resulting  $[\text{Ru}(\text{O})_3(\text{OH})]$  species is hydrogen-bonded to a second  $\text{AcOH}$  molecule to generate the active intermediate  $[\text{AcOH} \cdot \text{Ru}(\text{O})_3(\text{OH})]$  that oxidizes cyclohexane. The rate law is shown in eqn (8); at  $K'[\text{CH}_3\text{CO}_2\text{H}] \ll 1$ , the rate law becomes that of eqn (9).

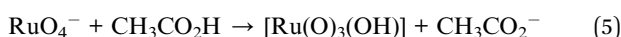


Fig. 4 (a) Effects of  $\text{CH}_3\text{CO}_2\text{H}$  on cyclohexane oxidation by  $\text{RuO}_4^-$  in  $\text{CH}_3\text{CN}$ . Conditions:  $[\text{Pr}_4\text{N}][\text{RuO}_4]$  (0.01 M), cyclohexane (1.0 M) in  $\text{CH}_3\text{CN}$  at 23 °C. (b) Plot of initial rate versus  $[\text{AcOH}]$  (slope =  $(2.72 \pm 0.13) \times 10^{-6}$ , y-intercept =  $-(3.33 \pm 3.82) \times 10^{-8}$ ,  $r = 0.9908$ ).



$$\text{Initial rate} = \frac{k'K'[\text{CH}_3\text{CO}_2\text{H}]}{1 + K'[\text{CH}_3\text{CO}_2\text{H}]} [\text{RuO}_4^-][\text{c-C}_6\text{H}_{12}] \quad (8)$$

$$\text{At } K'[\text{CH}_3\text{CO}_2\text{H}] \ll 1$$

$$\text{Initial rate} = k'K'[\text{AcOH}][\text{RuO}_4^-][\text{c-C}_6\text{H}_{12}] = k_{\text{AcOH}}[\text{AcOH}][\text{RuO}_4^-][\text{c-C}_6\text{H}_{12}] \quad (9)$$

From the slope of Fig. 4b and using  $[\text{RuO}_4^-] = 0.01 \text{ M}$  and  $[\text{c-C}_6\text{H}_{12}] = 1.0 \text{ M}$ ,  $k_{\text{AcOH}}$  is found to be  $(2.72 \pm 0.13) \times 10^{-4} \text{ M}^{-2} \text{ s}^{-1}$  at 23 °C.

#### Cooperative activating effects of metal ions and AcOH

Remarkably, when the oxidation of cyclohexane by  $\text{RuO}_4^-$  was carried out in the presence of  $\text{Ca}^{2+}$  and  $\text{AcOH}$ , both the rate and product yield were enhanced, as shown in Fig. 5. The amount of cyclohexanone produced by the  $\text{RuO}_4^-/\text{Ca}^{2+}/\text{AcOH}$  system is 38 mol%, compared with ca. 16 mol% by both  $\text{RuO}_4^-/\text{Ca}^{2+}$  and  $\text{RuO}_4^-/\text{AcOH}$  systems. In this case, the oxidation state of the ruthenium product was found to be +5 (see below, Fig. S3†), so this system functions as a two-electron oxidant and the actual yield is 76%, higher than the 64% using  $\text{Ca}^{2+}$  or  $\text{AcOH}$  alone.



Fig. 5 Time trace for cyclohexane oxidation by  $[\text{Pr}_4\text{N}][\text{RuO}_4]$  (0.01 M) in  $\text{CH}_3\text{CN}$  at 23 °C in the presence of (a) 1 equiv.  $\text{Ca}^{2+}$ , (b) 12 mol equiv. of  $\text{AcOH}$  and (c) 1 mol equiv.  $\text{Ca}^{2+}$  + 12 mol equiv.  $\text{AcOH}$ .



The yield of cyclohexanone was increased to 92% when the amount of acetic acid was increased to 250 equiv. ( $\text{CH}_3\text{CN}/\text{AcOH}$ : 6/1, Table 1). Note that in the absence of  $\text{Ca}(\text{OTf})_2$ , the yield of cyclohexanone did not increase with  $[\text{AcOH}]$ , as illustrated in Fig. 4a. Similar cooperative effects of  $\text{M}^{2+}$  and AcOH were also found for other group 2 ions (Table 1), with a maximum yield of 99% observed for  $\text{Sr}^{2+}/\text{AcOH}$ . However, no such cooperative effects were found for stronger Lewis acids such as  $\text{BF}_3$  and  $\text{Sc}(\text{OTf})_3$ , the yields remain the same in the absence or presence of AcOH. These results demonstrate the strong cooperative effects of relatively mild Brønsted and Lewis acid in activating a metal oxo species. Although the reaction rate is lower than that of  $\text{BF}_3$  or  $\text{Sc}(\text{OTf})_3$ , the Group 2 ion/AcOH combination is much more efficient in terms of product yield. Similar to the case of  $\text{CF}_3\text{SO}_3\text{H}$  discussed above, partial decomposition of  $\text{RuO}_4^-$  occurs in the presence of a strong Lewis acid, hence resulting in lower yields.

The kinetics of cyclohexane oxidation by  $\text{RuO}_4^-/\text{Ca}^{2+}/\text{AcOH}$  were investigated. Saturation kinetics were also observed when  $[\text{Ca}^{2+}]$  was increased (Fig. 6). Based on Fig. 6 and the mechanisms proposed above for  $\text{RuO}_4^-/\text{Ca}^{2+}$  and  $\text{RuO}_4^-/\text{AcOH}$ , the mechanism for this system can be represented by the following equations.



The rate-law is as shown in eqn (13):

$$\text{Initial rate} = \frac{k''K''[\text{Ca}(\text{OTf})_2]}{1 + K''[\text{Ca}(\text{OTf})_2]} [\text{RuO}_4^-][\text{AcOH}][\text{c} - \text{C}_6\text{H}_{12}] \quad (13)$$

**Table 1** Oxidation of cyclohexane by  $[\text{Pr}_4\text{N}][\text{RuO}_4^-]/\text{Lewis acid}$  in  $\text{CH}_3\text{CN}/\text{AcOH}$  (6:1, v/v)<sup>a</sup>

Entry <sup>a</sup>	Lewis acid	Yield of cyclohexanone <sup>d</sup> (%)	Time
1	$\text{Ca}(\text{OTf})_2$	92	5 h
2 <sup>b</sup>	$\text{Ca}(\text{OTf})_2$	92	5 h
3 <sup>c</sup>	$\text{Ca}(\text{OTf})_2$	91	5 h
4	$\text{Sr}(\text{OTf})_2$	99	5 h
5	$\text{Mg}(\text{OTf})_2$	86	5 h
6	$\text{Ba}(\text{OTf})_2$	86	5 h
7	$\text{BF}_3$	42	3 min
8	$\text{Sc}(\text{OTf})_3$	46	6 min

<sup>a</sup> Conditions:  $[\text{Pr}_4\text{N}][\text{RuO}_4^-]$ , 0.01 M; Lewis acid, 0.04 M; cyclohexane, 1.0 M; solvent,  $\text{CH}_3\text{CN}/\text{HOAc}$  (6:1, v/v); at 23 °C. <sup>b</sup> Under argon. <sup>c</sup> In the presence of 10 equiv. of  $\text{BrCCl}_3$ , only a trace amount of bromocyclohexane was detected. <sup>d</sup> Yield of cyclohexanone was calculated based on  $[\text{Pr}_4\text{N}][\text{RuO}_4^-]$  acting as two-electron oxidant. Yield = (mol of cyclohexanone)/(mol of  $[\text{Pr}_4\text{N}][\text{RuO}_4^-]$ )  $\times$  2  $\times$  100%, no cyclohexanol was detected.



**Fig. 6** (a) Plot of initial rate vs.  $[\text{Ca}^{2+}]$  for the  $\text{Ca}(\text{OTf})_2/\text{AcOH}$  activated oxidation of cyclohexane (0.10 M) by  $\text{RuO}_4^-$  (0.01 M) in  $\text{CH}_3\text{CN}$  at 23.0 °C. (b) The corresponding plot of  $1/\text{initial rate}$  vs.  $1/[\text{Ca}^{2+}]$ . Slope =  $(6.29 \pm 0.64) \times 10^3$ ,  $y$ -intercept =  $(1.29 \pm 0.09) \times 10^6$ ,  $r = 0.9504$ . Conditions:  $\text{RuO}_4^-$  (0.01 M); cyclohexane (1.0 M); AcOH (0.12 M);  $\text{Ca}(\text{OTf})_2$  (0.002 M – 0.040 M).

From eqn (11) and Fig. 6b,  $K''$  and  $k''$  are found to be  $(2.05 \pm 0.31) \times 10^2 \text{ M}^{-1}$  and  $(6.49 \pm 0.45) \times 10^{-4} \text{ M}^{-1} \text{ s}^{-1}$ , respectively.

A similar cooperative effect was also found for  $\text{Mg}^{2+}/\text{AcOH}$  (Fig. S4<sup>†</sup>). However, no increase in rate and yield were found for  $\text{Sc}^{3+}/\text{AcOH}$  (Fig. S5<sup>†</sup>).

### Ruthenium intermediates and products

Electrospray ionization mass spectrometry (ESI/MS) was employed to detect any intermediate formed between  $\text{RuO}_4^-$  and  $\text{Ca}^{2+}$ . The mass spectrum of  $[\text{Pr}_4\text{N}][\text{RuO}_4^-]$  in  $\text{CH}_3\text{CN}$  exhibits a single peak at  $m/z$  166.1 due to  $\text{RuO}_4^-$  (Fig. S6<sup>†</sup>). Upon addition of 0.25 equiv. of  $\text{Ca}(\text{OTf})_2$ , a new peak at  $m/z$  653.9 appeared, which is assigned to  $[\text{RuO}_4 \cdot \text{Ca}(\text{CF}_3\text{SO}_3)_2 \cdot \text{CF}_3\text{SO}_3\text{H}]^-$  (Fig. S7<sup>†</sup>). MS/MS of this ion ( $m/z$  653.9) gives fragment peaks due to  $\text{CF}_3\text{SO}_3^-$  ( $m/z$  148.9) and  $\text{RuO}_4^-$  ( $m/z = 165.9$ ) (Fig. S8<sup>†</sup>). This result provides evidence for the binding of  $\text{Ca}^{2+}$  to  $\text{RuO}_4^-$ .

The brown color of the solution of  $[\text{Pr}_4\text{N}][\text{RuO}_4^-]/\text{Ca}(\text{OTf})_2$  gradually lightened during cyclohexane oxidation, eventually a dark brown precipitate was observed and the solution became colorless. The dark precipitate, which is probably a  $\text{Ca}^{2+}$ -bridged polymeric species, was dissolved in 0.1 M  $\text{HNO}_3$  and the solution was titrated spectrophotometrically with the strong oxidant  $(\text{NH}_4)_2\text{Ce}(\text{NO}_3)_6$  (Ce(IV)). Upon addition of Ce(IV) to the ruthenium product solution, the characteristic vibronic-structured peaks at around 380 nm due to  $\text{RuO}_4^-$  appeared,<sup>26</sup> and  $2.3 \pm 0.3$  equiv. of Ce(IV) was consumed (Fig. S2<sup>†</sup>). This result indicates that the oxidation state of Ru in the dark brown product is +6 and hence the  $\text{Ca}^{2+}/\text{RuO}_4^-$  system acts as one-electron oxidant in the reaction with cyclohexane.

In cyclohexane oxidation by  $[\text{Pr}_4\text{N}][\text{RuO}_4^-]/\text{AcOH}$ , the brown solution gradually turned dark green but no precipitate was observed. ESI/MS of the dark green solution shows the appearance of a peak at  $m/z$  209 (Fig. S9<sup>†</sup>), which can be assigned to  $[\text{Ru}^{\text{VI}}\text{O}_3(\text{AcO})]^-$ . When  $\text{CH}_3\text{CO}_2\text{H}$  was replaced by  $\text{CD}_3\text{CO}_2\text{D}$ , the  $m/z$  209 peak was shifted to  $m/z$  212, indicating that the  $m/z$  209 peak consists of 1 AcO<sup>-</sup> ion. The assignment of +6 oxidation state to the ruthenium product is also supported by Ce(IV) titration, which consumes two equiv. of Ce(IV) to generate  $\text{RuO}_4^-$ . Hence the  $\text{RuO}_4^-/\text{AcOH}$  system also functions as a one-electron oxidant.



On the other hand, spectrophotometric titration of the product solution of  $\text{Ca}^{2+}/\text{AcOH}/\text{RuO}_4^-$  after cyclohexane oxidation shows that it consumes  $3.1 \pm 0.2$  equiv. of  $\text{Ce(IV)}$ , hence in this case the oxidation state of the Ru product is +5 and the system is a two-electron oxidant towards cyclohexane (Fig. S3†).

### Mechanistic studies

The same results were obtained for cyclohexane oxidation carried out under argon or air (Tables 1 and S2†). Also, the addition of  $\text{BrCCl}_3$ , a radical scavenger, had little effects on the oxidation of cyclohexane, and only a trace amount of bromocyclohexane was detected (Tables 1 and S2†). These results indicate that no freely diffusing alkyl radicals are formed in the oxidation of cyclohexane by  $\text{RuO}_4^-$  in the presence of  $\text{Ca}^{2+}$  and/or  $\text{AcOH}$ .

The kinetic isotope effects (KIE) for cyclohexane oxidation by  $\text{RuO}_4^-$  under various conditions were determined by competitive oxidation of an equimolar mixture of  $\text{c-C}_6\text{H}_{12}$  and  $\text{c-C}_6\text{D}_{12}$ . The KIE for  $\text{RuO}_4^-/\text{Ca}^{2+}$ ,  $\text{RuO}_4^-/\text{AcOH}$  and  $\text{RuO}_4^-/\text{Ca}^{2+}/\text{AcOH}$  were found to be  $6.4 \pm 0.2$ ,  $13.9 \pm 0.4$  and  $6.5 \pm 0.2$ , respectively. Such large KIEs are indicative of C–H bond cleavage in the rate-limiting step.

Based on the experimental results, the oxidation of alkane by  $\text{RuO}_4^-$  in the presence of Lewis acid (LA) appears to be consistent with a mechanism that involves the initial binding of LA to  $\text{RuO}_4^-$  to generate a precursor complex, which then reacts with alkane *via* a H-atom abstraction/O-rebound mechanism to generate the corresponding alcohol. Such a mechanism is commonly accepted for C–H bond activation by cytochrome P450 and various metal oxo species.<sup>30</sup> However, since only ketones are detected in the present case, this suggests that the initially formed alcohol is rapidly oxidized to give the ketone. This is supported by a competitive experiment involving the oxidation of a mixture of cyclohexane and cyclopentanol (10:1) by  $\text{RuO}_4^-/\text{Ca}^{2+}$ , which resulted in the rapid and exclusive formation of cyclopentanone (Fig. S10†). No alkene or products derived from its oxidation were observed in the oxidation of alkane by  $\text{RuO}_4^-/\text{Ca}^{2+}$ , which rules out a dehydrogenation mechanism that has been shown to occur in alkane oxidation by non-heme iron(IV) oxo species.<sup>31</sup> The binding of a Lewis acid to  $\text{RuO}_4^-$  enhances its oxidizing power, as observed in non-heme iron(IV) oxo complexes<sup>32</sup> and manganese oxo clusters.<sup>16,17</sup>

### Theoretical calculations

In order to obtain further insights into the activating effects of  $\text{Ca(II)}$  and  $\text{AcOH}$  on  $\text{RuO}_4^-$ , the reaction mechanisms for the oxidation of cyclohexane catalysed by  $\text{RuO}_4^-$  in the presence of  $\text{Ca(OTf)}_2$  and/or  $\text{AcOH}$  have been theoretically studied by density functional theory (DFT). As a comparison similar studies with  $\text{RuO}_4$  have also been carried out.

In the oxidation of cyclohexane by  $[\text{RuO}_4]^-$  in  $\text{CH}_3\text{CN}$  (Fig. 7), cyclohexane and  $[\text{RuO}_4]^-$  first form an intermediate,  $\text{INT1}(\text{RuO}_4^-)$ , in which the two species are weakly attracted together ( $[\text{RuO}_4 \cdots \text{C}_6\text{H}_{12}]^-$ ). HAT then occurs from  $\text{C}_6\text{H}_{12}$  to  $\text{Ru}=\text{O}$  *via* a transition state  $\text{TS1}(\text{RuO}_4^-)$  to form a second intermediate,  $\text{INT2}(\text{RuO}_4^-)$ . The reaction barrier ( $\Delta G_{298}^\ddagger$ ) for

the HAT is  $26.8 \text{ kcal mol}^{-1}$  in  $\text{CH}_3\text{CN}$ . Such a large  $\Delta G_{298}^\ddagger$  agrees with the experimental observation that  $\text{RuO}_4^-$  hardly reacts with cyclohexane at room temperature. The C1 of the cyclohexyl radical in  $\text{INT2}(\text{RuO}_4^-)$  bears  $-0.93$  electrons, consistent with a HAT process. The cyclohexyl radical then binds to another oxo ligand to generate an alkoxo intermediate  $[\text{RuO}_2(\text{OH})(\text{OC}_6\text{H}_{11})]^-$  *via*  $\text{TS2}(\text{RuO}_4^-)$ . It should be noted that the step after H-abstraction is not characterized as a rebound step, in contrast to cytochrome  $\text{P}_{450}$  and other mono-oxo species. Rather, another oxo group which is not used for H-atom abstraction combines with the carbon atom with a low barrier. Because of this reactivity pattern, a ruthenium-bound alkoxide instead of alcohol is formed as an intermediate. Then in the next step, proton transfer from  $\text{Ru}-\text{OH}$  to the alkoxide occurs *via*  $\text{TS3}(\text{RuO}_4^-)$  to generate the cyclohexanol product. Similar reaction pathways are observed for cyclohexane oxidation by  $\text{RuO}_4$ , except in this case no radical intermediate ( $\text{INT2}$ ) is formed (Fig. S11†). The reaction barrier ( $\Delta G_{298}^\ddagger$ ) is  $17.8 \text{ kcal mol}^{-1}$ , consistent with the experimental observation that  $\text{RuO}_4$  reacts readily with cyclohexane at room temperature.

In the oxidation of cyclohexane by  $\text{RuO}_4^-$  in the presence of  $[\text{Ca(OTf)}]^+$ , the reaction mechanism is similar.  $[\text{Ca(OTf)}]^+$  forms an intermediate,  $\text{INT1}(\text{CaOTf})$ , with  $\text{RuO}_4^-$ ; the Ca is bound to two oxo ligands. Due to the electron withdrawing effects of  $\text{Ca(II)}$  centre, the Ru–O bond lengths are changed from 1.740 (in  $\text{RuO}_4^-$ , Table S3†) to 1.775 (oxo bound to Ca) and 1.709 Å (free oxo) in  $\text{INT1}(\text{CaOTf})$ . HAT from  $\text{C}_6\text{H}_{12}$  then occurs *via* the shorter and more electrophilic  $\text{Ru}=\text{O}$  bond. In this case there is no cyclohexyl radical intermediate,  $\text{INT2}(\text{RuO}_4^-)$ ; HAT and binding of cyclohexyl radical to a second oxo occur in a single step. The  $\Delta G_{298}^\ddagger$  for the oxidation of cyclohexane by  $[\text{RuO}_4(\text{CaOTf})]$  (Fig. 7 and Table S3,† entry 3), *via*  $\text{TS1}(\text{CaOTf})$ , is  $18.5 \text{ kcal mol}^{-1}$ . Such a lowering of  $8.3 \text{ kcal mol}^{-1}$  is in agreement with the observed accelerating effect of  $\text{Ca(II)}$ . We have also found the  $\Delta G_{298}^\ddagger$  for the oxidation of cyclohexane by  $[\text{RuO}_4(\text{Ca})]^+$  (Table S3,† entry 5) is higher than that by  $[\text{RuO}_4(\text{CaOTf})]$ , so  $[\text{RuO}_4(\text{Ca})]^+$  should not be the active species in the oxidation of cyclohexane.

In the presence of acetic acid,  $\text{RuO}_4^-$  is protonated to give  $\text{INT1}(\text{AcOH})$ ,  $[\text{RuO}_3\text{OH}(\text{AcO}) \cdots \text{C}_6\text{H}_{12}]$ . The  $\text{AcO}^-$  is held by two additional  $\text{AcOH}$  molecules through hydrogen bonding (structures given in Table S3†). The Ru–OH bond distance is 1.858 Å; protonation results in shortening of two of the  $\text{Ru}=\text{O}$  from 1.740 Å (in  $\text{RuO}_4^-$ ) to 1.709 Å. HAT by  $\text{INT1}(\text{AcOH})$  occurs *via* one of the shorter and more electrophilic  $\text{Ru}=\text{O}$ ; the resulting cyclohexyl radical then binds to  $\text{Ru}-\text{OH} \cdots \text{OAc}$  to generate Ru bound cyclohexanol in the same step,  $\text{INT2}(\text{AcOH})$ . The  $\Delta G_{298}^\ddagger$  for HAT from  $\text{C}_6\text{H}_{12}$  to  $\text{INT1}(\text{AcOH})$  *via*  $\text{TS1}(\text{AcOH})$  is  $15.2 \text{ kcal mol}^{-1}$ , which is significantly lower than the  $\Delta G_{298}^\ddagger$  for  $\text{RuO}_4^-$  alone by  $11.6 \text{ kcal mol}^{-1}$ , in accordance with the experimentally observed accelerating effects of  $\text{AcOH}$  on  $\text{RuO}_4^-$ .

In the presence of both  $[\text{CaOTf}]^+$  and  $\text{AcOH}$ , the intermediate with  $\text{RuO}_4^-$ ,  $\text{INT1}(\text{CaOTf} + \text{AcOH})$ , consists of  $\text{AcO}^-$  and Ca forming a chelate ring with  $\text{Ru}=\text{O}$  and  $\text{Ru}-\text{OH}$ , as well as three H-bonded  $\text{AcOH}$  molecules (Fig. 7 and Table S3,† entry 4). The free  $\text{Ru}=\text{O}$  bonds are further shortened to 1.692 Å. Accordingly





Fig. 7 PESs for cyclohexane oxidation by  $[\text{RuO}_4]^-/[\text{RuO}_4(\text{AcOH})]^-/[\text{RuO}_4(\text{CaOTf})]/[\text{RuO}_4(\text{AcOH})(\text{CaOTf})]$  at the B3LYP level using LanL2TZ(f) basis set (Ru) and 6–311+G(d,p) basis set (non-metals). Relative 298 K Gibbs free energies in acetonitrile are given in  $\text{kcal mol}^{-1}$ . Not all acetic acid molecules are shown for simplicity.

the  $\Delta G_{298}^\ddagger$  for HAT from cyclohexane *via*  $\text{TS1}(\text{CaOTf} + \text{AcOH})$  is lowered to  $10.8 \text{ kcal mol}^{-1}$ , which is smaller than the value of  $18.5 \text{ kcal mol}^{-1}$  and  $15.2 \text{ kcal mol}^{-1}$ , respectively, with  $\text{Ca}(\text{OTf})^+$  or  $\text{AcOH}$  alone. This is in agreement with the observed cooperative activating effects of  $\text{AcOH}$  and  $\text{Ca}(\text{II})$ . HAT and binding of the resulting cyclohexyl radical to a Ca-bound oxo ligand occur in one step. Protonation by Ru–OH to the alkoxide then occurs to generate cyclohexanol. The potential energy surfaces (PES) for  $\text{RuO}_4/\text{Ca}(\text{OTf})^+$ ,  $\text{RuO}_4/\text{AcOH}$  and  $\text{RuO}_4/\text{Ca}(\text{OTf})^+/\text{AcOH}$  are shown in Fig. S11.† The  $\Delta G_{298}^\ddagger$  for HAT by  $\text{RuO}_4$  alone is  $17.8 \text{ kcal mol}^{-1}$ , consistent with the experimental observation that  $\text{RuO}_4$  is able to oxidize cyclohexane at ambient conditions. There are little or no changes in the Ru=O distances of  $\text{RuO}_4$  upon binding to  $\text{Ca}(\text{OTf})^+$  and/or  $\text{AcOH}$ , and there are only small changes in the reaction barriers, in agreement with experimental observations. This is in accordance with the Ru=O bonds being highly electrophilic and non-basic, hence there is little affinity for Lewis acids.

## Conclusions

Our results demonstrate a remarkable cooperative effect of a weak Brønsted acid and a weak Lewis acid on the activation of a metal oxo species.  $\text{RuO}_4^-$ , although in high oxidation state of +VII, is a weak oxidant due to stabilization by the four oxo ligands. However, it can be readily activated by a mild Lewis

acid such as  $\text{Ca}^{2+}$  or other group II metal ions, as well as a weak Brønsted acid such as  $\text{CH}_3\text{CO}_2\text{H}$ . The addition of both  $\text{Ca}^{2+}$  and  $\text{CH}_3\text{CO}_2\text{H}$  generates a highly efficient system that can oxidize unactivated C–H bonds with much higher yields than the use of strong Lewis acids such as  $\text{Sc}^{3+}$  or  $\text{BF}_3$ , with or without  $\text{CH}_3\text{CO}_2\text{H}$ . Such an observation may provide insights into the design of active oxidants based on metal oxo species in combination with relatively weak Brønsted and Lewis acids, especially if the metal oxo or the substrate is sensitive to strong acids. Our studies may also be relevant to oxidation by metal oxo species in biological systems, where only mild Brønsted acids such as alkanolic or amino acids, and mild Lewis acids such as  $\text{Zn}^{2+}$  or  $\text{Ca}^{2+}$ , are present in cells. So may be highly efficient oxidizing systems can be generated in biological systems using this strategy.

## Conflicts of interest

There are no conflicts to declare.

## Acknowledgements

This work was supported by the Hong Kong Research Grants Council (CityU 11336816), the National Science Foundation of China (21975043) and Guangdong Provincial Key Platforms and Major Scientific Research Projects for Colleges and Universities



(2018KTSCX227). We thank Dr Hajime Hirao for very helpful discussions.

## Notes and references

- 1 T. Devi, Y.-M. Lee, W. Nam and S. Fukuzumi, *Coord. Chem. Rev.*, 2020, **410**, 213219.
- 2 Y. Liu and T.-C. Lau, *J. Am. Chem. Soc.*, 2019, **141**, 3755–3766.
- 3 S. Fukuzumi, *Coord. Chem. Rev.*, 2013, **257**, 1564–1575.
- 4 D. J. Vinyard, G. M. Ananyev and G. C. Dismukes, *Annu. Rev. Biochem.*, 2013, **82**, 577–606.
- 5 J. Yano and V. Yachandra, *Chem. Rev.*, 2014, **114**, 4175–4205.
- 6 J. D. Blakemore, R. H. Crabtree and G. W. Brudvig, *Chem. Rev.*, 2015, **115**, 12974–13005.
- 7 J. Barber, *Chem. Soc. Rev.*, 2009, **38**, 185–196.
- 8 Y. Umena, K. Kawakami, J.-R. Shen and N. Kamiya, *Nature*, 2011, **473**, 55–60.
- 9 K. M. Davis, B. T. Sullivan, M. C. Palenik, L. Yan, V. Purohit, G. Robison, I. Kosheleva, R. W. Henning, G. T. Seidler and Y. Pushkar, *Phys. Rev. X*, 2018, **8**, 041014.
- 10 Y. Pushkar, K. M. Davis and M. C. Palenik, *J. Phys. Chem. Lett.*, 2018, **9**, 3525–3531.
- 11 W. W. Y. Lam, S.-M. Yiu, J. M. N. Lee, S. K.-Y. Yau, H.-K. Kwong, T.-C. Lau, D. Liu and Z. Lin, *J. Am. Chem. Soc.*, 2006, **128**, 2851–2858.
- 12 Y. Morimoto, H. Kotani, J. Park, Y.-M. Lee, W. Nam and S. Fukuzumi, *J. Am. Chem. Soc.*, 2011, **133**, 403–405.
- 13 H. Yoon, H. Yoon, Y.-M. Lee, X. Wu, K.-B. Cho, R. Sarangi, W. Nam and F. S. Fukuzumi, *J. Am. Chem. Soc.*, 2013, **135**, 9186–9194.
- 14 T. Devi, Y.-M. Lee, W. Nam and S. Fukuzumi, *J. Am. Chem. Soc.*, 2020, **142**, 365–372.
- 15 T. Devi, Y.-M. Lee, W. Nam and S. Fukuzumi, *J. Am. Chem. Soc.*, 2018, **140**, 8372–8375.
- 16 E. Y. Tsui, R. Tran, J. Yano and T. Agapie, *Nat. Chem.*, 2013, **5**, 293–299.
- 17 E. Y. Tsui and T. Agapie, *Proc. Natl. Acad. Sci. U.S.A.*, 2013, **110**, 10084–10088.
- 18 M. M. Najafpour, T. Ehrenberg, M. Wiechen and P. Kurz, *Angew. Chem., Int. Ed.*, 2010, **49**, 2233–2237.
- 19 M. Wiechen, I. Zaharieva, H. Dau and P. Kurz, *Chem. Sci.*, 2012, **3**, 2330–2339.
- 20 S. Bang, Y.-M. Lee, S. Hong, K.-B. Cho, Y. Nishida, M. S. Seo, R. Sarangi, S. Fukuzumi and W. Nam, *Nat. Chem.*, 2014, **6**, 934–940.
- 21 H. Du, Po-K. Lo, Z. Hu, H. Liang, K.-C. Lau, Y.-N. Wang, W. W. Y. Lam and T.-C. Lau, *Chem. Commun.*, 2011, **47**, 7143–7145.
- 22 L. Ma, W. W. Y. Lam, P.-K. Lo, K.-C. Lau and T.-C. Lau, *Angew. Chem., Int. Ed.*, 2016, **55**, 3012–3016.
- 23 T.-C. Lau and C.-K. Mak, *J. Chem. Soc., Chem. Commun.*, 1993, 766–767.
- 24 S.-M. Yiu, Z.-B. Wu, C.-K. Mak and T.-C. Lau, *J. Am. Chem. Soc.*, 2004, **126**, 14921–14929.
- 25 S.-M. Yiu, W.-L. Man, X. Wang, W. W. Y. Lam, S.-M. Ng, H.-K. Kwong, K.-C. Lau and T.-C. Lau, *Chem. Commun.*, 2011, **47**, 4159–4161.
- 26 W. P. Griffith, *Ruthenium Oxidation Complexes: Their Uses as Homogenous Organic Catalysts*, Springer, 2011.
- 27 W. P. Griffith, S. V. Ley, G. P. Whitcombe and A. D. White, *J. Chem. Soc., Chem. Commun.*, 1987, 1625–1627.
- 28 S. J. Hawkes, *J. Chem. Educ.*, 1996, **73**, 516.
- 29 E. A. Seddon and K. R. Seddon, *The Chemistry of Ruthenium*, Elsevier, Amsterdam, 1984, vol. 52.
- 30 J. L. McLain, J. Lee and J. T. Groves, *Biomimetic Oxidations Catalyzed by Transition Metal Complexes*. Imperial College Press, London, 2000.
- 31 K.-B. Cho, X. Wu, Y.-M. Lee, Y. H. Kwon, S. Shaik and W. Nam, *J. Am. Chem. Soc.*, 2012, **134**, 20222–20225.
- 32 W. Nam, Y.-M. Lee and S. Fukuzumi, *Acc. Chem. Res.*, 2014, **47**, 1146–1154.

